

Article

Selective Flotation Behavior of Dolomite from Fluorapatite Using Hydroxy Ethylene Diphosphonic Acid as High-Efficiency Depressant

Jingkun Zhang, Zhiyun Xiao * and Hongbo Zhang *

College of Mining, Inner Mongolia University of Technology, Hohhot 010000, China

* Correspondence: a45579801@163.com (Z.X.); hongbozhang123456@163.com (H.Z.)

Abstract: In the reverse flotation of fluorapatite and dolomite, high-efficiency depressors of fluorapatite have received considerable attention. In this paper, the depression mechanism of hydroxy ethylene diphosphonic acid (HEDP) was studied for the first time as a novel fluorapatite depressant on the surface of fluorapatite. The effect of HEDP on the flotation behavior of the two minerals was studied by single and mixed minerals in flotation tests. HEDP exhibited an excellent depression effect on fluorapatite flotation, whereas its adsorption on dolomite surface was minimal. Fluorapatite and dolomite were effectively separated by applying sodium oleate as a collector and HEDP as a depressant at pH 6.0. The depression mechanism of HEDP on fluorapatite was further analyzed via contact angle measurement, zeta potential and X-ray photoelectron spectroscopic (XPS) analysis. We found that HEDP seriously hindered the adsorption of sodium oleate (NaOL) on the fluorapatite surface and had a minimal effect on the dolomite surface. XPS analysis results indicate that the strong adsorption of HEDP on the fluorapatite surface can be attributed to the strong chelation between the electron-rich groups of HEDP and Ca ions on the fluorapatite surface. Therefore, HEDP is used as a selective depressant of fluorapatite in the fluorapatite–dolomite flotation–separation process.

Keywords: HEDP; fluorapatite; flotation; depression mechanism



Citation: Zhang, J.; Xiao, Z.; Zhang, H. Selective Flotation Behavior of Dolomite from Fluorapatite Using Hydroxy Ethylene Diphosphonic Acid as High-Efficiency Depressant. *Minerals* **2022**, *12*, 1633. <https://doi.org/10.3390/min12121633>

Received: 7 November 2022

Accepted: 29 November 2022

Published: 19 December 2022

Publisher's Note: MDPI stays neutral with regard to jurisdictional claims in published maps and institutional affiliations.



Copyright: © 2022 by the authors. Licensee MDPI, Basel, Switzerland. This article is an open access article distributed under the terms and conditions of the Creative Commons Attribution (CC BY) license (<https://creativecommons.org/licenses/by/4.0/>).

1. Introduction

Phosphorus is one of the most common elements on Earth and is essential for life. It is widely used in industrial processes, such as the production of fertilizer, detergents, fluxes and cement. Nevertheless, with the development of the global economy, the demand for phosphorus is gradually increasing, leading to a global shortage phosphate resource production. Therefore, phosphate resources have been listed as strategic resources by some countries, including the European Union, making their effective development and utilization increasingly important. In addition, the increasing demand for phosphorus has led to a sharp decrease in the reserves of high-grade phosphorus resources; therefore, it is urgent to promote new technologies of phosphorus enrichment from low-grade phosphorus resources. In such ores, the main valuable mineral, fluorapatite, is usually associated with calcium–magnesium gangue minerals or calcium–silicon gangue minerals, such as dolomite, calcite and quartz. Froth flotation, as the most extensive method in mineral processing, is widely used to separate fluorapatite and gangue minerals. However, there are some difficulties associated with flotation of dolomite from apatite because the surfaces of apatite and dolomite have similar active calcium sites [1]. Therefore, they are similarly reactive to traditional fatty acid collectors, resulting in low flotation efficiency and reduced phosphate concentrate grades. This increases the subsequent production costs of the phosphorus chemical industry. Thus, it is important to develop more effective flotation separation technology for apatite and dolomite in order to obtain high-grade phosphate rock products.

Accordingly, in order to effectively separate apatite from dolomite, many studies have focused on the development of new selective flotation reagents. In recent decades, many researchers have attempted to exploit novel collectors to improve flotation recovery, such as benzohydroxamic acid (BHA) [2], Oleic acid mixed with linoleic acid and linolenic acid collector [3], pataua palm tree oil [4,5], sodium dodecyl sulfonate (SDS) mixed with a fatty acid collector [6], saponified gutter oil fatty acid [7], oleic acid amide [8], modified mineral oil [9], jojoba oil [10], oleamide–sodium dodecyl benzene sulfonate [11] and cottonseed oil [12]. However, considering the cost and economic applicability, these new collectors are still not applicable. Therefore, traditional fatty acid collectors and fatty acid derivatives are still currently used in industrial applications. Furthermore, the addition of fatty acid collectors alone cannot increase the difference in floatability, so it is difficult to separate apatite from dolomite by flotation. Related studies have shown that fatty acid collectors can enhance the hydrophobicity and floatability of apatite and dolomite in combination with active sites on mineral surfaces to form calcium oleate and magnesium oleate. Therefore, in order to effectively use phosphate resources, the development of effective depressants is very important to increase the floatability difference between apatite and dolomite and to achieve the selective separation of apatite and carbonate gangue minerals. Many apatite depressants have been reported to date, such as sulfuric acid [1,13], phosphoric acid [14,15], sodium pyrophosphate [16,17], citric acid [18], thiophosphoric acid [19], waste acid [20], etc. Thiophosphoric acid has been widely used as an apatite depressant owing to its wide range of sources and low unit cost.

However, the high consumption of sulfuric acid and phosphoric acid produces acidic wastewater and corrodes flotation equipment. In addition, the production of calcium sulfate and calcium phosphate in sediments can lead to pipeline obstruction, which is an issue that has not been solved yet. Therefore, the separation of apatite from dolomite by a mixture of sulfuric acid and phosphoric acid remains a serious problem.

To the best of our knowledge, 1-hydroxyethylene-1, 1-diphosphonic acid (HEDP) is a non-toxic and environmentally friendly organic phosphonic acid compound [21]. As a representative of organic phosphonates, HEDP is a quaternary acid and chelating agent that is relatively inexpensive and readily available. Because the HEDP structure contains twin phosphonate groups, it has an excellent affinity for various metal ions [21], and this group has a variety of strong interactions with metal ions. Therefore, HEDP has been widely used in metal corrosion, protection and water treatment fields. HEDP can form insoluble deposits with Fe^{3+} on the metal surface by dissolving the oxidized components on the metal surface to prevent metal corrosion [22–25]. The key to the ability of HEDP to prevent scale formation is its ability to delay or prevent material precipitation and avoid scale formation on metal surfaces by chelating with Ca^{2+} , Mg^{2+} and Zn^{2+} [26–30]. Therefore, HEDP has attracted attention as a flotation reagent in mineral flotation separation. Some scholars have found that HEDP, as a collector of chalcopyrite, can obtain chalcopyrite by flotation from pyrite [31]. HEDP has also been proven to be a suitable fluorite depressant, and fluorite can be separated from calcite by reverse flotation [32]. However, HEDP has not been reported for flotation separation of apatite and dolomite minerals. In addition, apatite and dolomite have similar Ca^{2+} active sites on cleavage planes to which they are normally exposed. Therefore, how HEDP selectively separates apatite from dolomite remains unclear.

In this study, the flotation behavior of apatite and dolomite was investigated by flotation tests of single and mixed minerals. Single flotation experiments show that HEDP is an effective fluorapatite depressant. In addition, a zeta potential test, contact angle measurement and X-ray photoelectron spectroscopic (XPS) analysis were further used to elucidate the selective inhibition mechanism of HEDP on fluorapatite in the flotation separation of dolomite and fluorapatite. This study provides theoretical guidance for selective flotation of dolomite from fluorapatite.

2. Materials and Methods

2.1. Materials and Reagents

High-purity mineral crystals come from a mine in Guizhou Province, China. After two kinds of minerals were broken in a crusher, they were selected and purified by hand and ground manually in a ceramic mortar. After grinding, the product was sieved to a given size ($-75 \mu\text{m} + 38 \mu\text{m}$) for microflotation experiments. As shown in Figure 1, XRD results indicate almost no impurities in the samples, meeting the requirements of this experimental study. In addition, the mineral samples were ground in a mortar to less than $5 \mu\text{m}$ for zeta potential measurement and XPS analysis. Sodium oleate (NaOl , $\text{C}_{18}\text{H}_{33}\text{O}_2\text{Na}$, Analytical grade, 97%) purchased from Aladdin was used as a collector. 1-hydroxyethylene-1,1-diphosphonic acid (HEDP, $\text{C}_2\text{H}_8\text{O}_7\text{P}_2$, industrial grade, 97%) from Shandong Taihe Technologies Co., Ltd. (Zaozhuang, China) was employed as the depressant. The molecular formula of sodium oleate and HEDP is shown in the figure. Sodium hydroxide (NaOH , analytical grade, 99%) and hydrochloric acid (HCl , analytical grade, 37%) purchased from Tianjin, China, were dissolved in deionized water. Sodium hydroxide and hydrochloric acid solutions were obtained to adjust the pH of pulp. Potassium chloride (KCl , analytical grade, 99.5%) purchased from Sinopharmaceutics group was prepared to a given concentration (1%) for zeta potential measurement. Deionized water with resistivity of more than $18 \text{ M } \omega \text{ cm}^{-1}$ was used for the experiment.

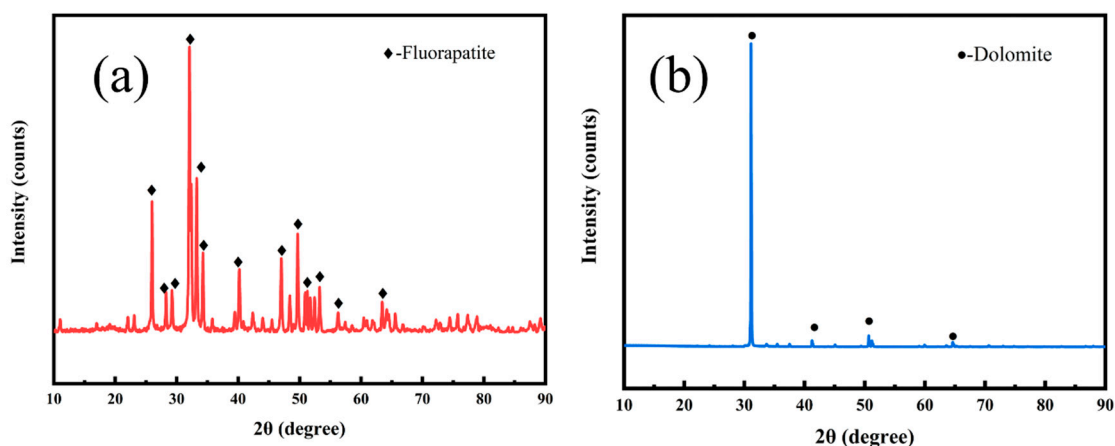


Figure 1. XRD patterns of fluorapatite (a) and dolomite (b) minerals used in the experiment.

2.2. Microflotation Experiments

A single-mineral flotation experiment was conducted with fluorapatite and dolomite on a 40 mL XFG-II flotation machine (Jilin Exploration Machinery Factory, Changchun, China) with the spindle speed set at 1992 r/min. Flotation pulp was obtained by adding 2 g single mineral or mixed mineral (1.2 g fluorapatite and 0.8 g dolomite) and 35 mL deionized water to the flotation tank. In order to achieve full mixing, the pulp was stirred for 1 min. Then, according to the flotation experiment flow sheet (Figure 2), flotation reagents were successively added into the solution for a flotation test. After scraping, filtering, drying and weighing, concentrate and tailings were obtained. After drying and filtering, the recovery of single mineral flotation test product was calculated directly according to weight. Each flotation experiment was carried out at least three times under the same experimental conditions, and the average value was calculated and reported.

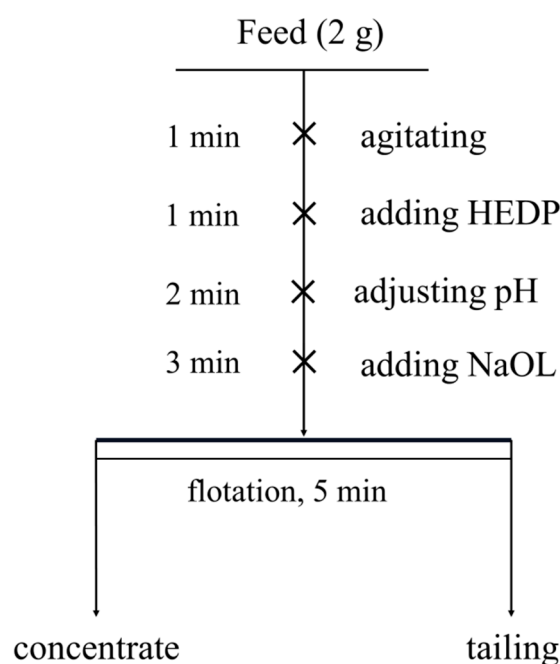


Figure 2. Flow sheet of single-mineral flotation experiment.

2.3. Wettability Analysis

The mineral surface contact angle affects floatability, so the mineral surface contact angle can be measured to determine mineral floatability. In this study, in order to measure the contact Angle, block fluorapatite and dolomite were polished smooth by sandpaper with varying mesh numbers. Before the contact angle was measured, the mineral surface was repeatedly cleaned with distilled water in order to remove contaminants on the mineral surface. The surface treatment conditions of fluorapatite and dolomite with different reagents were the same as the flotation test conditions. After treatment, the surface was cleaned with deionized water and dried with nitrogen. The contact angle was measured on a HARKE-SPCA-X contact angle measuring instrument (HARKE-SPCA-X3, Beijing HARKE Instrument Pilot Factory, Beijing, China). A drop of distilled water was dropped on the mineral surface to form a stable droplet, and the contact angle was measured using the baseline circle method. Three measurements were taken at different locations, and the average value was calculated for each contact angle measurement. Furthermore, the standard error of each test was calculated and represented by an error bar.

2.4. Zeta Potential Measurement

Zeta potentials of minerals were measured by a Zeta Sizer Nano ZS90 (Malvern Panalytical Co., Ltd., Malvern, UK) at 25 °C. Prior to use for zeta potential measurements, mineral samples were ground in an agate mortar to less than 5 µm. For each measurement, 0.04 g of sample was added to a 50 mL beaker with 40 mL of KCl solution at a concentration of 1×10^{-3} mol/L. Then, according to the flotation experimental conditions, flotation agents were added, and the pH of solution was adjusted. The solution was stirred for 10 min, then allowed to stand for 5 min to precipitate large particles in the suspension. An appropriate amount of supernatant was extracted for zeta potential measurement. All zeta potential tests were repeated three times, and the mean and standard errors were calculated.

2.5. X-ray Photoelectron Spectroscopic Analysis

X-ray photoelectron spectroscopy (XPS) was used to detect changes in the chemical environment of HEDP- and NaOL-treated mineral samples. All XPS analyses were performed on a ESCALAB 250 Xi spectrometer (Thermo Scientific Co., Ltd. Waltham, MA, USA) equipped with a monochrome Al-K α source of 6 mA and 12 KV. In the process of

sample preparation, mineral samples were treated with different reagents according to the conditions described for the flotation test; then, the suspension was filtered, washed and dried for XPS analysis. Finally, Avantage software was used to fit the peaks of XPS spectra, and all binding energies were corrected by pollutant carbon ($C_{1s} = 284.6$ eV).

3. Results and Discussion

3.1. Microflotation Experiments

The effect of collector dosage on the flotation behavior of fluorapatite and dolomite was studied by microflotation test. The experimental results of flotation are shown in Figure 3, illustrating the relationship between the flotation recovery of fluorapatite and dolomite and the dosage of NaOL.

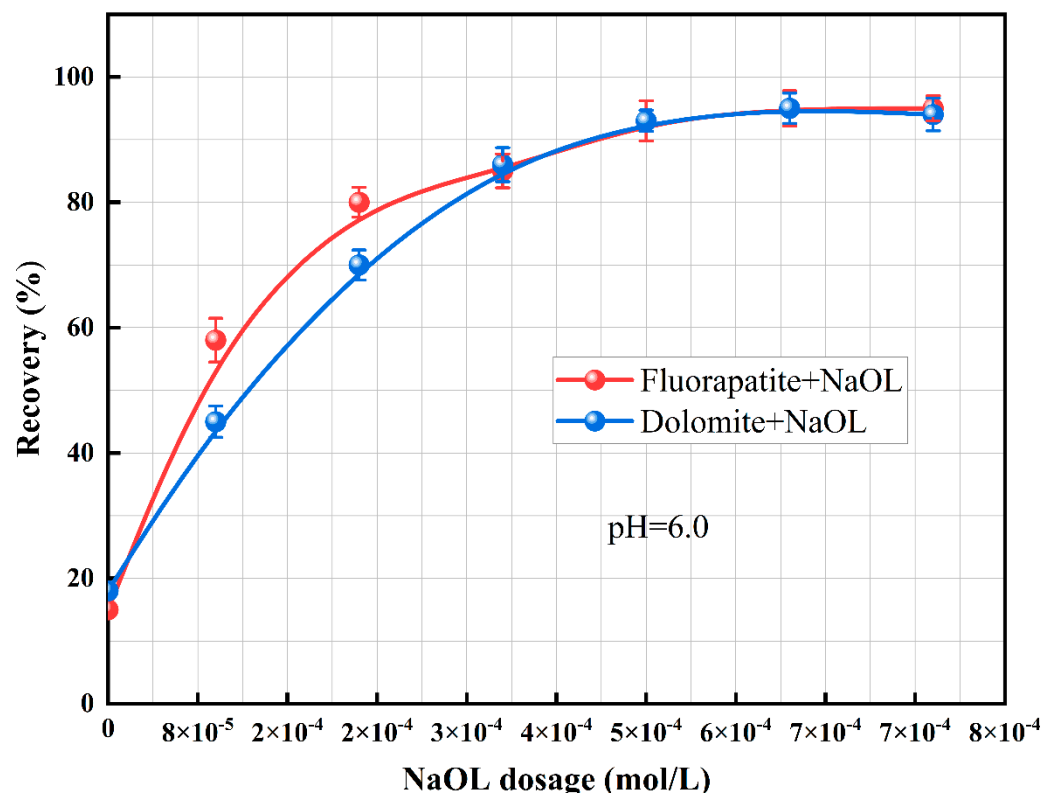


Figure 3. Influence of collector dosage on flotation recovery of fluorapatite and dolomite.

As shown in Figure 3, the two minerals do not achieve improved recovery rates at low collector dosage, owing to their poor natural floatability. Figure 3 also shows that the recovery rate of the two minerals increases gradually with an increased amount of collector. For fluorapatite and dolomite, when the amount of collector reaches 5×10^{-4} mol/L, the flotation recovery is more than 90%, indicating that NaOL has a good collection ability for fluorapatite and dolomite. The recovery curves of the two minerals show that the recovery of fluorapatite is always higher than that of dolomite because the floatability of fluorapatite is higher than that of dolomite. In addition, the flotation results show that the optimal amount of collector is 5×10^{-4} mol/L, and depressants need to be added for the separation of fluorapatite and dolomite.

We further studied the effect of depressants on the flotation behavior of fluorapatite and dolomite by micro flotation test. Figure 4 indicates that with the addition of NaOL, fluorapatite recovery decreased significantly with increased HEDP dosage. When the HEDP dosage was 3×10^{-5} mol/L, fluorapatite was significantly depressed, and the recovery was 1%. On the other hand, dolomite maintained good floatability, with a recovery of 94%. With increased HEDP dosage, the recovery of fluorapatite remained unchanged below 5%, whereas the recovery of dolomite remained above 90%. In addition, the separation of

fluorapatite and dolomite can be achieved with a small amount of HEDP, indicating that HEDP is highly selective and valuable for industrial applications.

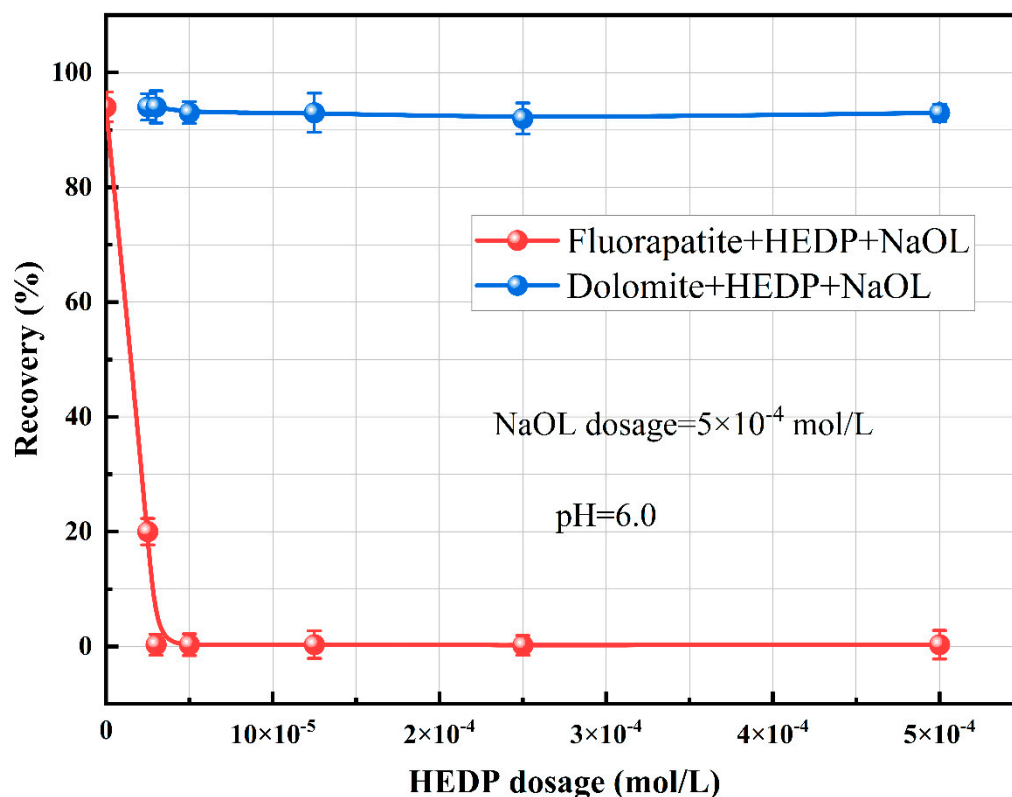


Figure 4. Influence of depressant dosage on the flotation recovery of fluorapatite and dolomite.

The effect of slurry pH on the flotation behavior of fluorapatite and dolomite was further investigated with the addition of various reagents. Figure 5 shows the relationship between the recovery of various minerals and pulp pH with or without the addition of HEDP. The results show that when NaOL was added alone, pulp pH had little influence on the flotation behavior of fluorapatite and dolomite. Both fluorapatite and dolomite show high floatability across the pH range, with recovery of both minerals remaining above 90%. When both HEDP and NaOL were added, HEDP had a considerable depression effect on fluorapatite in the whole measured pH range. Furthermore, the pH value has a considerable influence on the flotation recovery of dolomite, with high recovery (>90%) in the range of 5 to 7.5; however, when the pulp pH value was greater than 7.5, the dolomite recovery decreased significantly. At pH 8, the recovery of dolomite decreased to 26%. Figure 5 shows that at pH 6, the difference between the flotation recovery of fluorapatite and that of dolomite reached the maximum, so pulp pH 6 was selected as the optimal pH value for flotation separation of fluorapatite and dolomite.

Considering that HEDP has excellent selective depression ability on fluorapatite, apatite and dolomite exhibit considerable differences in floatability. We further explored the excellent selection performance of HEDP by artificial mixed mineral flotation experiments at pH 6, the results of which are presented in Figure 6. When fluorapatite and dolomite were mixed at a mass ratio of 3:2, the grade of P_2O_5 was 21%. When NaOL was added, the grade of fluorapatite in the flotation concentrate was 26%, and the recovery of fluorapatite was 36.5% in the absence of HEDP. These results indicate that without the addition of HEDP, the flotation separation efficiency of the two minerals was poor, and the grade of fluorapatite did not meet the industrial requirements. When 3×10^{-5} mol/L HEDP was added, the apatite grade in the flotation concentrate increased to 33%, and the apatite recovery increased to 92.5%. The results of artificial mixed mineral flotation experiments

prove that HEDP can effectively separate apatite and dolomite, with potential for use as a novel apatite depressant.

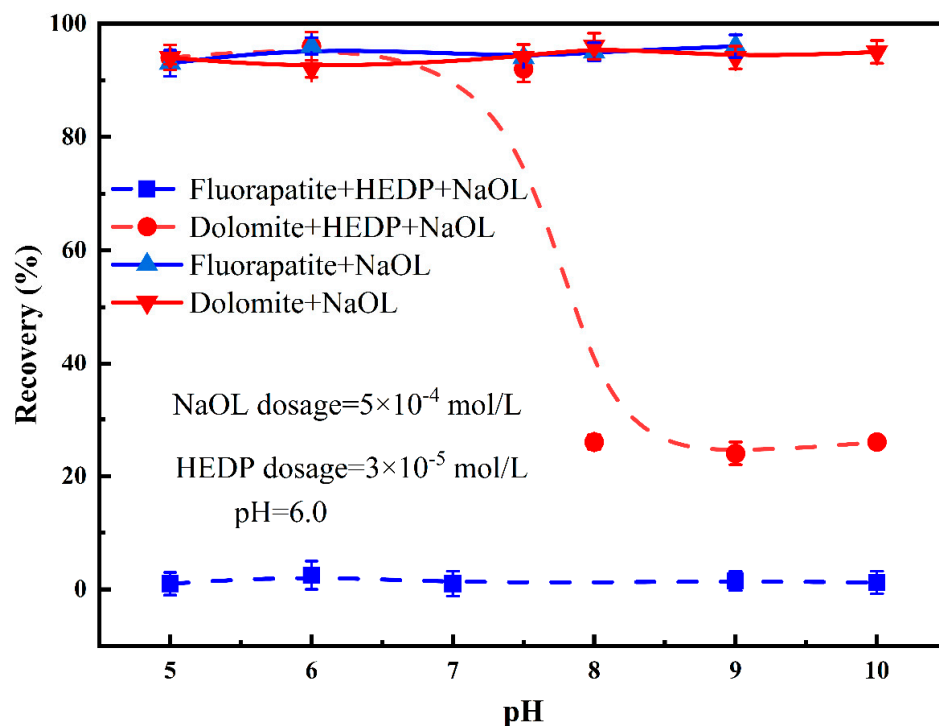


Figure 5. Influence of pH on flotation behavior of fluorapatite and dolomite with and without the addition of HEDP in the presence of NaOL.

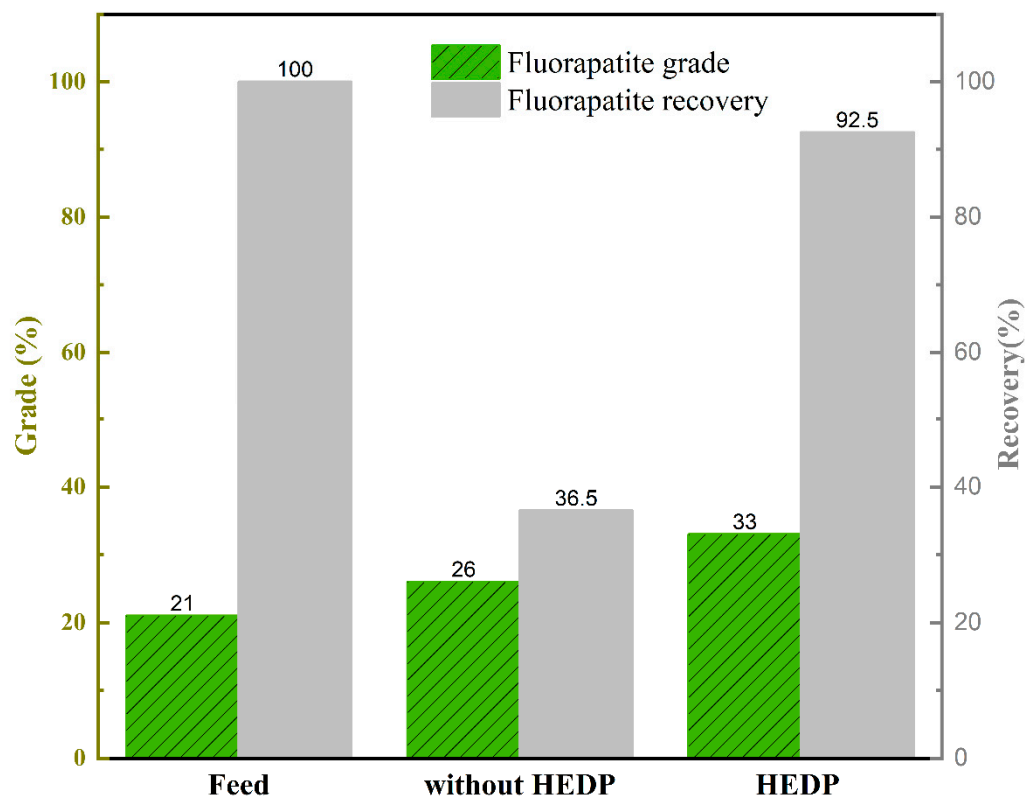


Figure 6. Phosphorus concentrates grade and recovery under the reaction of various reagents in artificial mixed-mineral experiments.

3.2. Wettability Analysis

The microflotation test results have proven that HEDP has excellent depression ability on fluorapatite, so dolomite can be separated from fluorapatite via flotation methods. At present, it is generally believed that the effect of reagent separation is closely related to its effect on mineral surface hydrophobicity [33]. Generally speaking, the contact angle reflecting the hydrophobicity of a mineral surface has been widely used to study differences in mineral flotation behavior caused by the addition of flotation agents. Therefore, we measured the surface contact angle of different minerals with and without the addition of flotation reagents. The measurement results are presented in Figure 7. The contact angles of fluorapatite and dolomite were 60° and 50°, respectively, when no flotation reagent was added, proving the poor hydrophobicity of fluorapatite and dolomite. The contact angles of fluorapatite and dolomite increased significantly with the addition of NaOL, reaching 85° and 83°, respectively. The experimental results demonstrate that NaOL can enhance the hydrophobicity of a mineral surface, so the two minerals showed high floatability after adding NaOL alone. When additional HEDP added to fluorapatite and dolomite, the surface of the dolomite maintained high hydrophobicity, with a contact angle of 83°. The measurement results show that the preaddition of HEDP does not affect the adsorption of NaOL on the surface of dolomite, which is consistent with the result of high recovery of dolomite in the flotation experiment. However, compared with dolomite, the surface hydrophobicity of fluorapatite treated with HEDP and NaOL differed significantly from that of fluorapatite treated with NaOL alone, with a contact angle of 48°, which is much smaller than that of fluorapatite treated with NaOL alone.

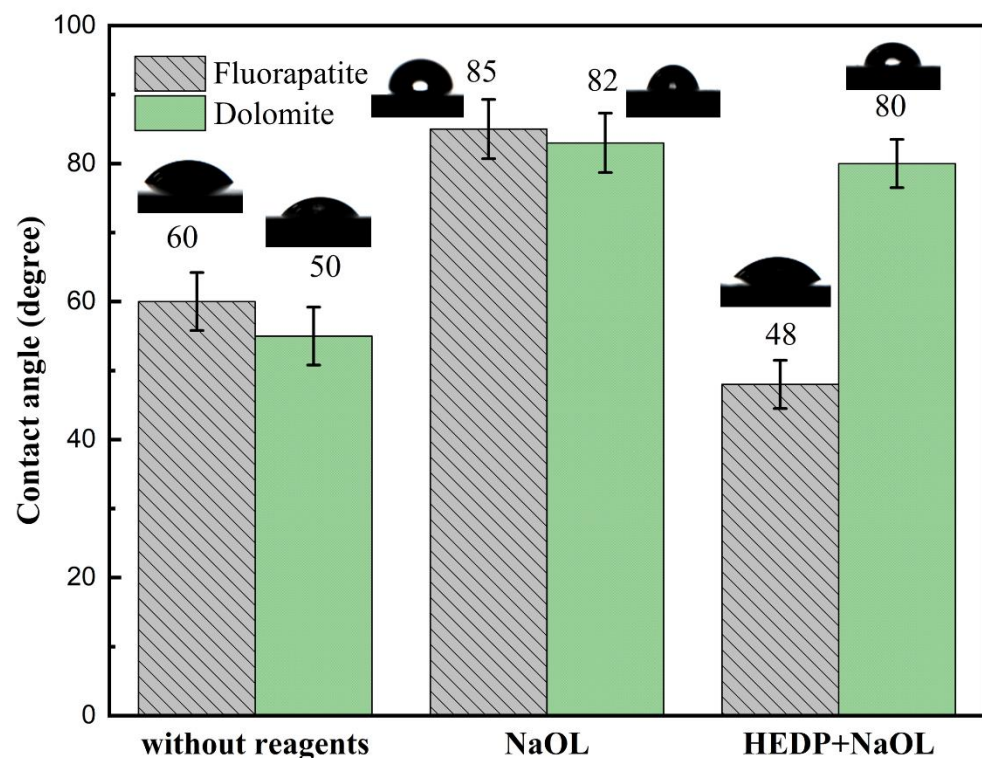


Figure 7. Contact angles of fluorapatite and dolomite under the reaction of HEDP and NaOL (HEDP: 3×10^{-5} mol/L; NaOL: 5×10^{-4} mol/L; pH = 6.0).

3.3. Zeta Potential Measurements

We further studied the mechanism of reverse flotation separation of dolomite from fluorapatite by measuring the zeta potential; the results are shown in Figure 8. The zeta potential of fluorapatite with and without HEDP as a function of pH is shown in Figure 8a. In the pH range of 5–11, the Zeta potential of pure fluorapatite decreases with

the increase in pH, and no isoelectric point is detected in the whole pH range, which is match with the results of previous studies [19,34]. The Zeta potential of fluorapatite decreased significantly after the addition of HEDP, indicating that HEDP strongly adsorb on the surface of fluorapatite. A significant shift of 24 mV (-5 mV to -29 mV) occurs at pH 6.0, which is related to the absorption of negatively charged HEDP onto the fluorapatite surface. When both HEDP and NaOL were introduced, the zeta potential of fluorapatite decreased from -29 mV to -30 mV at pH 6.0. It can be seen that the Zeta potential curve of fluorapatite treated with HEDP and NaOL is not significantly different from that treated with HEDP alone, indicating that the pre-adsorption of HEDP greatly obstructs the adsorption of NaOL on the surface of fluorapatite. Therefore, the floatability of fluorapatite is poor in the presence of HEDP.

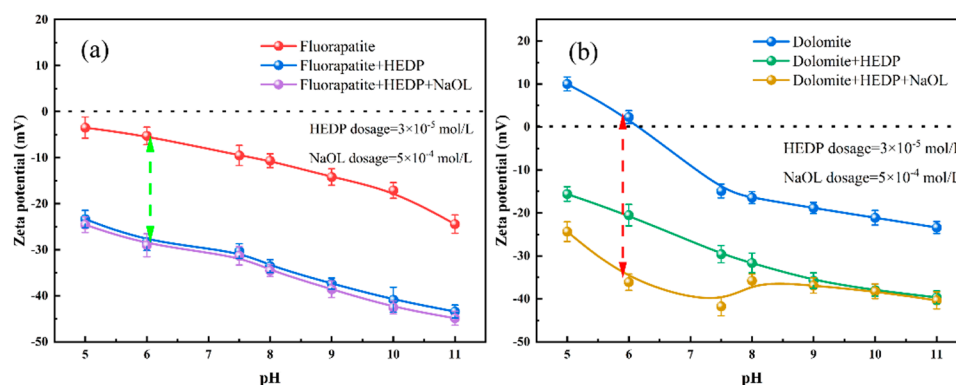


Figure 8. Zeta potentials of fluorapatite (a) and dolomite (b) treated with HEDP and NaOL at varying pH values (HEDP: 3×10^{-5} mol/L; NaOL: 5×10^{-4} mol/L). red line: Zeta potential decline of fluorapatite under different conditions; Green line: Zeta potential decline of dolomite under different conditions.

Zeta potential of dolomite with different reagents was shown in Figure 8b. The zeta potential of dolomite decreases with increased pH, and its isoelectric point appears around pH 6.5. This is consistent with previous literature reports [19,35]. The zeta potential of dolomite decreased slowly, indicating that HEDP was absorbed on the surface after its addition. However, there is a considerable difference between the zeta potential dolomite and fluorapatite. The decline of dolomite is less than that of fluorapatite. For dolomite, the zeta potential was only reduced by 18 mV at pH 6.0. After further addition of NaOL, the zeta potential of dolomite continued to significantly decrease by 15 mV at pH 6.0, indicating that HEDP has weak adsorption capacity on the surface of dolomite, so NaOL can be adsorbed on the surface of dolomite after HEDP treatment, maintaining floatability under the condition of HEDP preadsorption. According to Yang's research [36], the recovery of dolomite continues to decrease until the pH is less than 8. When the pH is greater than 8, the recovery rate of dolomite is very low. This is consistent with our research. The inhibition effect of HEDP on dolomite is considerably affected by pH.

3.4. XPS Analysis

To further reveal the adsorption mechanism of HEDP and NaOL with fluorapatite and dolomite, the surface composition and chemical states of minerals before and after HEDP and NaOL addition were analyzed by XPS test. Figure 9 shows the full spectrum of XPS before and after the surface interaction of HEDP with fluorapatite and dolomite.

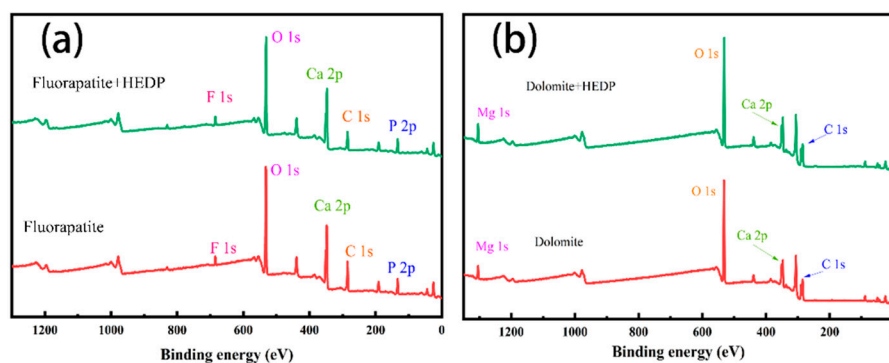


Figure 9. XPS wide-scan spectra of fluorapatite (a) and dolomite (b) before and after reaction with HEDP and NaOL.

As shown in Figure 8a, for fluorapatite without any agent, significant peaks (O1s, C1s, Ca2p, P1s and F1s) were observed throughout the spectrum. After HEDP treatment, the concentration of P element on the fluorapatite surface increased significantly, which may be related to the adsorption of HEDP on the fluorapatite surface. As shown in Figure 9b, peaks Mg1s, C1s, Ca2p and O1s occur on the surface of dolomite without any treatment. On the contrary, no peak of P element was found on the surface of dolomite after the action of HEDP. This result indicates that the interaction of HEDP on the surface of dolomite is weak or there is no interaction, i.e., lower than the detection limit of the XPS analysis instrument, so P element is not detected on the surface of dolomite.

In order to clarify the changes in the concentration of main elements on the surface of the two minerals before and after HEDP, the changes in composition and content of main elements are summarized in Table 1. As shown in Table 1, after HEDP treatment, the concentration of P element in fluorapatite increased by 0.75% compared with the initial surface concentration of fluorapatite without any treatment. However, P element was not found on the surface of dolomite, indicating that the adsorption of P element on the surface of fluorapatite is stronger than that on the surface of dolomite

Table 1. Atomic concentrations of main elements on fluorapatite and dolomite surfaces treated with HEDP at pH 6.

Samples	Atomic Concentration (%)				
	C1s	O1s	Ca2p	P2p	F1s
Fluorapatite	26.47	44.80	15.98	10.06	2.69
Fluorapatite + HEDP	24.45	47.18	13.93	10.81	3.63
Samples	Atomic Concentration (%)				
	C1s	O1s	Ca2p	Mg1s	—
Dolomite	38.32	48.91	9.16	3.61	—
Dolomite + HEDP	38.30	47.56	9.66	4.48	—

The narrow spectrum of elements obtained by XPS test was used to further reveal the interaction mechanism of HEDP and NaOL with fluorapatite and dolomite. Metal-active sites exposed to mineral surfaces have been reported to dominate the interactions between minerals and various reagents [36]. Therefore, we performed a peak-fitting analysis on the narrow spectrum of Ca element and P element in fluorapatite, the results of which are shown in Figure 10. As shown in Figure 10a, for bare fluorapatite, double peaks of Ca 2P appear at 347.64 eV and 351.17 eV, which correspond to Ca 2p_{3/2} and Ca 2p_{1/2} orbits of fluorapatite, respectively [37]. After HEDP treatment, Ca 2P peaks of fluorapatite shifted to 347.73 eV and 351.30 eV, respectively. Compared with bare fluorapatite, the binding energy decreased by 0.11 eV and 0.13 eV, respectively. Moreover, two new peaks appeared at 347.59 eV and 350.90 eV, corresponding to RPO₃-Ca. Similarly, after the interaction

of fluorapatite with HEDP, the binding energy of P 2p changed considerably, shifting from 133.68 eV to 133.42 eV (Figure 10b). The above analysis results indicate that the surface chemical environment of HEDP-treated fluorapatite changed considerably due to the chelation between HEDP and Ca sites on the fluorapatite surface.

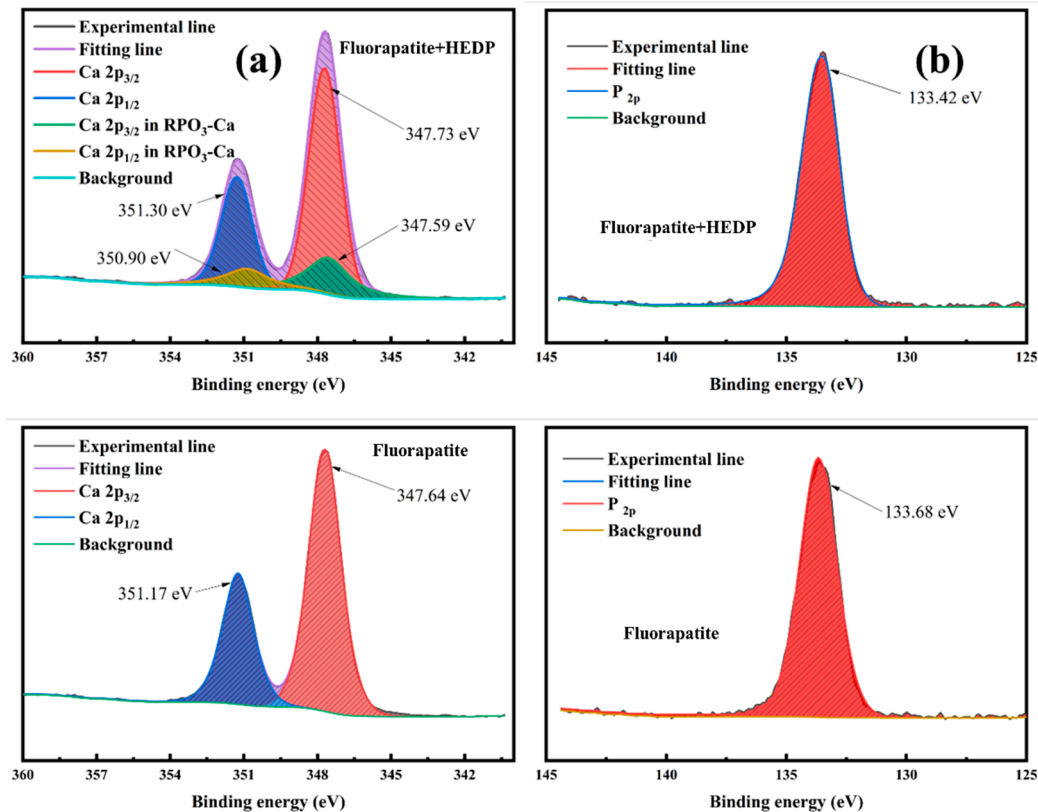


Figure 10. XPS spectra of Ca 2p (a) and P_{2p} (b) for fluorapatite before and after the interaction with HEDP.

Figure 11 shows the narrow spectrum and peak fitting of Ca and Mg of dolomite. As shown in Figure 11a, the Ca 2P peaks of bare dolomite are located at 347.45 eV and 350.96 eV, which are attributed to Ca 2p_{3/2} and Ca 2P_{1/2} of dolomite, respectively. After HEDP treatment, the Ca2p binding energy of dolomite moved from 347.38 eV and 350.84 eV and from 0.07 eV to 0.06 eV, respectively. Similarly, the binding energy of Mg1s for bare dolomite shifted from 1304.4 eV to 1304.35 eV (see Figure 11b). Small changes in the binding energy of Ca2p and Mg1s indicate that HEDP has weak interaction with the active sites of Ca and Mg on the surface of dolomite, resulting in almost no adsorption of HEDP on the surface of dolomite.

In addition to the chemical adsorption between HEDP and calcium sites on the surface of fluorapatite, HEDP has three OH groups, which can be adsorbed on the surface of fluorapatite and dolomite through hydrogen bonding. For example, -OH...Fs on the surface of fluorapatite and -OH...Os on the surface of dolomite, as well as the F atom on the surface of fluorapatite, have higher electronegativity and a smaller atomic radius than the O atom on the surface of dolomite [32,38]. In addition, the average hydrogen bond energy of -OH...Fs is 98 kJ/mol, whereas that of -OH...Os is only 21 kJ/mol [39]. These results show that the hydrogen bonding between HEDP and fluorapatite is greater than that between HEDP and dolomite.

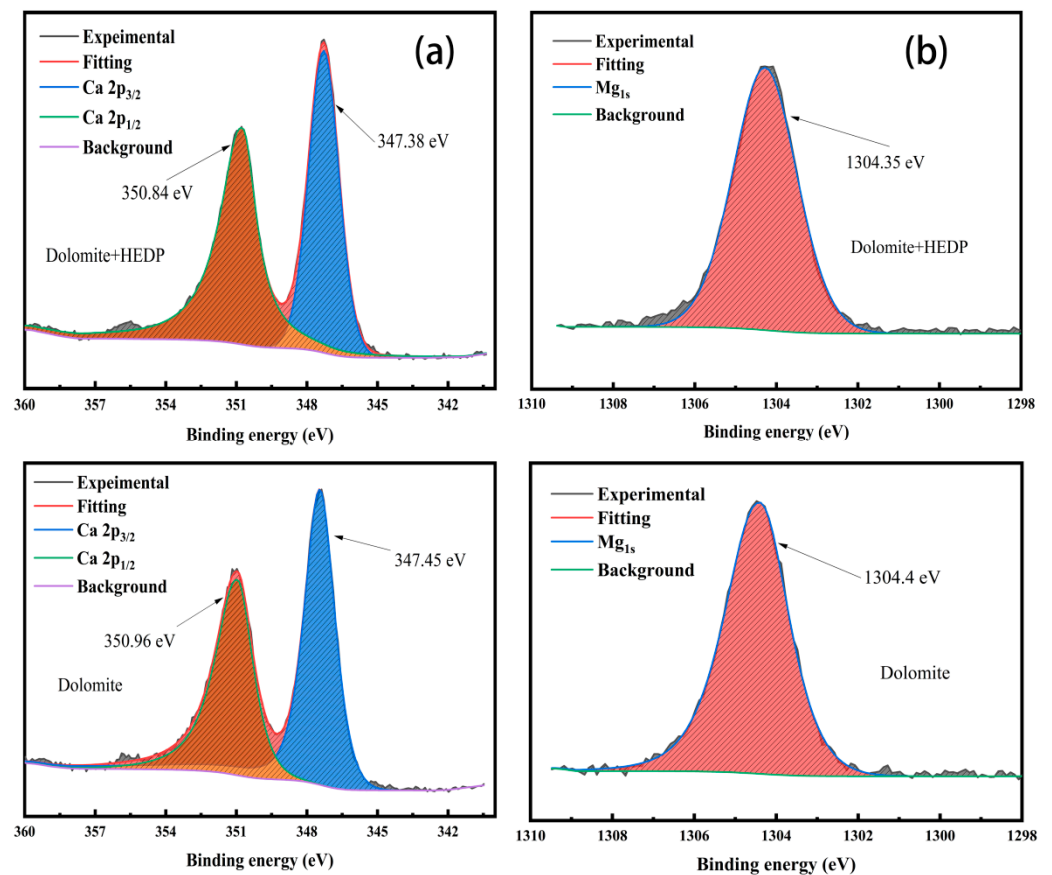


Figure 11. XPS spectrum of Ca 1s (a) and Mg 1s (b) for dolomite before and after the interaction with HEDP.

Generally speaking, the action mechanism of organic matter on a mineral surface is divided into chemical complexation, electrostatic interaction, hydrogen bonding and hydrophobic interaction. In conclusion, a series of tests and analysis results confirm that HEDP formed stable RPO_3-Ca on the surface of fluorapatite by chelating the $R-PO_3$ group with a calcium site on the surface of fluorapatite. Moreover, the hydrogen bond interaction between the F atom and calcium site on the surface of fluorapatite enhances the adsorption. For dolomite, HEDP is mainly adsorbed on the dolomite surface by a weak hydrogen bond, so the adsorption strength of HEDP on the dolomite surface is weak. Therefore, after the action of HEDP, the collector can bind to the Ca site on the dolomite surface and adsorb on the dolomite surface. Therefore, in the flotation process, dolomite has good floatability due to surface hydrophobicity and bubble adhesion, whereas the fluorapatite surface is difficult to adhere to bubbles, owing to hydrophilicity, resulting in poor floatability.

Finally, combining the above analysis results, we propose a possible mechanism map. As shown in Figure 12, under the optimal conditions of the flotation experiment, the binding ability of HEDP to dolomite surface-active sites is weak, so NaOL can be adsorbed on the dolomite surface to enhance its hydrophobicity. On the contrary, the calcium-active sites on the fluorapatite surface have a strong chelating ability with HEDP, so HEDP occupies the calcium-active sites on the fluorapatite surface. Owing to the weak adsorption of NaOL on the surface of fluorapatite, fluorapatite has poor hydrophobicity and is difficult to float.

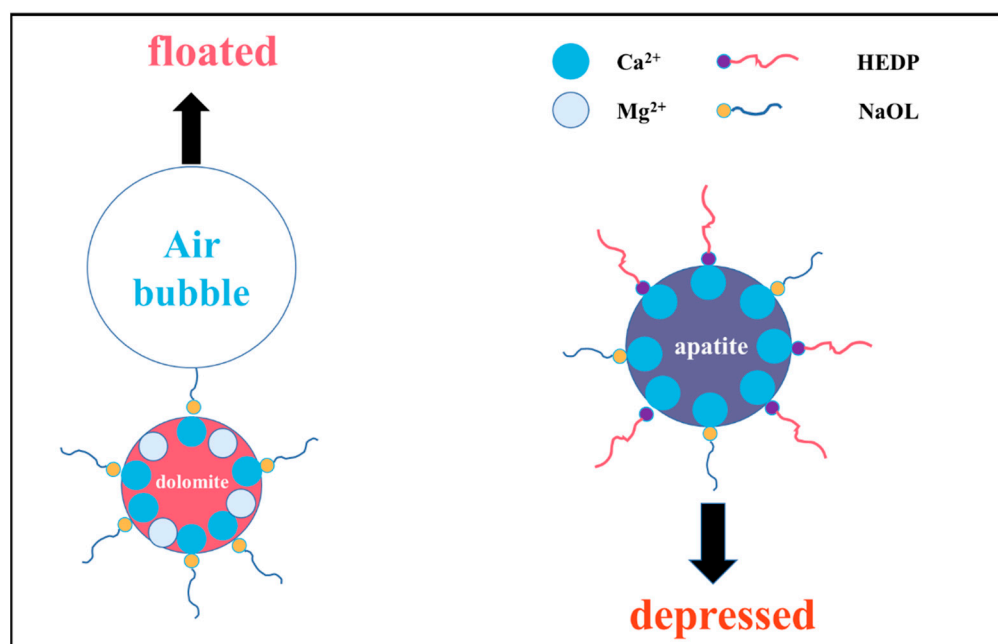


Figure 12. Schematic diagram of possible flotation separation mechanism of dolomite and fluorapatite at pH 6.0.

4. Conclusions

In the present study, HEDP was employed as fluorapatite depressant to improve the flotation separation effect of dolomite and fluorapatite for the first time. The inhibition mechanism of HEDP on fluorapatite was studied in a single flotation experiment and artificial mixed-minerals flotation experiments, as well as using a contact angle measurement, zeta potential test and XPS test. The results of the single-mineral flotation test and artificial mixed-mineral flotation tests illustrate that under the conditions of pH 6.0, NaOL of 5×10^{-4} mol/L and HEDP of 3×10^{-5} mol/L, HEDP can achieve the selective separation of fluorapatite and dolomite. The addition of HEDP can effectively inhibit fluorapatite floating, whereas dolomite is almost unaffected. Zeta potential and XPS analyses show that HEDP can adsorb on both fluorapatite and dolomite surfaces, with a high matching degree of HEDP and fluorapatite surface Ca sites, forming cyclic chelate ($\text{Ca}_2(\text{HEDP})$), which occupies the active site of NaOL adsorption on the surface of fluorapatite, whereas HEDP has weak matching ability with the active site on the surface of dolomite, so it is difficult to adsorb on the surface of dolomite. Therefore, the floatability of dolomite treated by HEDP is still high. In general, HEDP causes the difference in the action between fluorapatite surface and dolomite surface and NaOL, achieving the selective flotation separation of fluorapatite and dolomite. Because HEDP has the advantages of low dosage and high selectivity, it is of considerable significance for the industrial application of phosphate ore reverse flotation. The inhibition mechanism of HEDP on fluorapatite at pH 6.0 was systematically investigated in this study; however, the inhibition mechanism of HEDP on dolomite was not systematically studied.

Author Contributions: Conceptualization, J.Z. and Z.X.; methodology, J.Z.; software, J.Z.; writing—original draft preparation, J.Z.; writing—review and editing, J.Z.; supervision, Z.X. and H.Z.; funding acquisition, H.Z. All authors have read and agreed to the published version of the manuscript.

Funding: This research was funded by [Inner Mongolia Autonomous Region Key Technology Project] grant number [2020GG0266].

Conflicts of Interest: The authors declare that they have no conflict of interest.

References

1. Zou, H.; Cao, Q.; Liu, D.; Yu, X.; Lai, H. Surface Features of Fluorapatite and Dolomite in the Reverse Flotation Process Using Sulfuric Acid as a Depressor. *Minerals* **2019**, *9*, 33. [\[CrossRef\]](#)
2. Wang, L.; Tian, M.; Khoso, S.A.; Hu, Y.; Sun, W.; Gao, Z. Improved Flotation Separation of Apatite from Calcite with Benzohydroxamic Acid Collector. *Miner. Processing Extr. Metall. Rev.* **2019**, *40*, 427–436. [\[CrossRef\]](#)
3. Cao, Q.; Cheng, J.; Wen, S.; Li, C.; Bai, S.; Liu, D. A mixed collector system for phosphate flotation. *Miner. Eng.* **2015**, *78*, 114–121. [\[CrossRef\]](#)
4. De Oliveira, P.; Mansur, H.; Mansur, A.; da Silva, G.; Peres, A.E.C. Apatite flotation using pataua palm tree oil as collector. *J. Mater. Res. Technol.* **2019**, *8*, 4612–4619. [\[CrossRef\]](#)
5. De Carvalho, J.A.E.; Brandão, P.R.G.; Henriques, A.B.; de Oliveira, P.S.; Cançado, R.Z.L.; da Silva, G.R. Selective flotation of apatite from micaceous minerals using pataua palm tree oil collector. *Miner. Eng.* **2020**, *156*, 106474. [\[CrossRef\]](#)
6. Cao, Q.; Cheng, J.; Wen, S.; Li, C.; Liu, J. Synergistic effect of dodecyl sulfonate on apatite flotation with fatty acid collector. *Sep. Sci. Technol.* **2016**, *51*, 1389–1396. [\[CrossRef\]](#)
7. Liu, X.; Li, C.; Luo, H.; Cheng, R.; Liu, F. Selective reverse flotation of apatite from dolomite in collophanite ore using saponified gutter oil fatty acid as a collector. *Int. J. Miner. Processing* **2017**, *165*, 20–27. [\[CrossRef\]](#)
8. Jong, K.; Han, Y.; Ryom, S. Flotation mechanism of oleic acid amide on apatite. *Colloids Surf. A Physicochem. Eng. Asp.* **2017**, *523*, 127–131. [\[CrossRef\]](#)
9. Wei, K.; Liu, W.; Peng, X.; Liu, W.; Naixu, Z.; Li, Z. Investigating flotation behavior and mechanism of modified mineral oil in the separation of apatite ore. *Physicochem. Probl. Miner. Process.* **2020**, *56*, 471–482. [\[CrossRef\]](#)
10. Santos, E.P.; Dutra, A.J.B.; Oliveira, J.F. The effect of jojoba oil on the surface properties of calcite and apatite aiming at their selective flotation. *Int. J. Miner. Process.* **2015**, *143*, 34–38. [\[CrossRef\]](#)
11. Ding, Z.; Li, J.; Bi, Y.; Yu, P.; Dai, H.; Wen, S.; Bai, S. The adsorption mechanism of synergic reagents and its effect on apatite flotation in oleamide-sodium dodecyl benzene sulfonate (SDBS) system. *Miner. Eng.* **2021**, *170*, 107070. [\[CrossRef\]](#)
12. Ruan, Y.; Zhang, Z.; Luo, H.; Xiao, C.; Zhou, F.; Chi, R. Ambient Temperature Flotation of Sedimentary Phosphate Ore Using Cottonseed Oil as a Collector. *Minerals* **2017**, *7*, 65. [\[CrossRef\]](#)
13. Cao, Q.; Zou, H.; Chen, X.; Yu, X. Interaction of sulfuric acid with dolomite (104) surface and its impact on the adsorption of oleate anion: A DFT study. *Physicochem. Probl. Miner. Process.* **2020**, *56*, 34–42.
14. Liu, X.; Ruan, Y.; Li, C.; Cheng, R. Effect and mechanism of phosphoric acid in the apatite/dolomite flotation system. *Int. J. Miner. Process.* **2017**, *167*, 95–102. [\[CrossRef\]](#)
15. Chen, Q.; Zhang, Q.; Hart, B.R.; Ye, J. Study on the effect of collector and inhibitor acid on the floatability of collophane and dolomite in acidic media by TOF-SIMS and XPS. *Surf. Interface Anal.* **2020**, *52*, 355–363. [\[CrossRef\]](#)
16. Pan, Z.; Wang, Y.; Wei, Q.; Chen, X.; Jiao, F.; Qin, W. Effect of sodium pyrophosphate on the flotation separation of calcite from apatite. *Sep. Purif. Technol.* **2020**, *242*, 116408. [\[CrossRef\]](#)
17. Pan, Z.; Wang, Y.; Wang, Y.; Jiao, F.; Qin, W. Understanding the depression mechanism of sodium citrate on apatite flotation. *Colloids Surf. A Physicochem. Eng. Asp.* **2020**, *588*, 124312. [\[CrossRef\]](#)
18. Liu, X.; Luo, H.; Cheng, R.; Li, C.; Zhang, J. Effect of citric acid and flotation performance of combined depressant on collophanite ore. *Miner. Eng.* **2017**, *109*, 162–168. [\[CrossRef\]](#)
19. Zhang, H.; Zhou, F.; Liu, M.; Jin, Y.; Xiao, L.; Yu, H. Employing sulfur–phosphorus mixed acid as a depressant: A novel investigation in flotation of collophanite. *Energy Sources Part A Recovery Util. Environ. Eff.* **2020**, 1–14. [\[CrossRef\]](#)
20. Chen, Y.; Wu, J.; Liu, R.; Liu, C.; Liu, L.; Li, R.; Zhang, H.; Pang, J.; Liu, D. Application of waste acid from phosphogypsum dam as an eco-friendly depressant in collophane flotation. *J. Clean. Prod.* **2020**, *267*, 122184. [\[CrossRef\]](#)
21. Kornev, V.I.; Kropacheva, T.N.; Sorokina, U.V. Coordination compounds of oxovanadium (IV) with organophosphonic complexes in aqueous solutions. *Russ. J. Inorg. Chem.* **2015**, *60*, 403–408. [\[CrossRef\]](#)
22. Moudgil, H.K.; Yadav, S.; Chaudhary, R.S.; Kumar, D. Synergistic effect of some antiscalants as corrosion inhibitor for industrial cooling water system. *J. Appl. Electrochem.* **2009**, *39*, 1339–1347. [\[CrossRef\]](#)
23. Scarazzato, T.; Buzzi, D.C.; Bernardes, A.M.; Espinosa, D.C.R. Treatment of wastewaters from cyanide-free plating process by electrodialysis. *J. Clean. Prod.* **2015**, *91*, 241–250. [\[CrossRef\]](#)
24. Kumar, H.; Chaudhary, R.S. Inhibitive action of 1-hydroxyethylenedine-1,1-diphosphonic acid antiscalant towards corrosion of carbon steel in cooling water system. *J. Indian Chem. Soc.* **2011**, *88*, 1589–1598.
25. Wang, D.; Yang, J.; Xue, F.; Wang, J.; Hu, W. Experimental and computational study of zinc coordinated 1-hydroxyethylidene-1,1-diphosphonic acid self-assembled film on steel surface. *Colloids Surf. A Physicochem. Eng. Asp.* **2020**, *612*, 126009. [\[CrossRef\]](#)
26. Zeng, B.; Li, M.-D.; Zhu, Z.-P.; Zhao, J.-M.; Zhang, H. Application of 1-hydroxyethylidene-1, 1-diphosphonic acid in boiler water for industrial boilers. *Water Sci. Technol.* **2013**, *67*, 1544–1550. [\[CrossRef\]](#) [\[PubMed\]](#)
27. Boulahlib-Bendaoud, Y.; Ghizellaoui, S. Use of The HEDP For the Inhibition of The Tartar of Ground Waters. *Energy Procedia* **2012**, *18*, 1501–1510. [\[CrossRef\]](#)
28. Khormali, A.; Petrakov, D.G.; Moghaddam, R.N. Study of adsorption/desorption properties of a new scale inhibitor package to prevent calcium carbonate formation during water injection in oil reservoirs. *J. Pet. Sci. Eng.* **2017**, *153*, 257–267. [\[CrossRef\]](#)

29. Huang, N.; Wang, W.-L.; Xu, Z.-B.; Wu, Q.-Y.; Hu, H.-Y. UV/chlorine oxidation of the phosphonate antiscalant 1-Hydroxyethane-1,1-diphosphonic acid (HEDP) used for reverse osmosis processes: Organic phosphorus removal and scale inhibition properties changes. *J. Environ. Manag.* **2019**, *237*, 180–186. [[CrossRef](#)]
30. Abd-El-Khalek, D.E.; Abd-El-Nabey, B.A.; Abdel-kawi, M.A.; Ebrahim, S.; Ramadan, S.R. The inhibition of crystal growth of gypsum and barite scales in industrial systems using green antiscalant. *Water Supply* **2019**, *19*, 2140–2146. [[CrossRef](#)]
31. Huang, Z.; Wang, J.; Sun, W.; Hu, Y.; Cao, J.; Gao, Z. Selective flotation of chalcopyrite from pyrite using diphosphonic acid as collector. *Miner. Eng.* **2019**, *140*, 105890. [[CrossRef](#)]
32. Wang, J.; Li, W.; Zhou, Z.; Gao, Z.; Hu, Y.; Sun, W. 1-Hydroxyethylidene-1,1-diphosphonic acid used as pH-dependent switch to depress and activate fluorite flotation I: Depressing behavior and mechanism. *Chem. Eng. Sci.* **2020**, *214*, 115369. [[CrossRef](#)]
33. Dong, L.; Jiao, F.; Qin, W.; Zhu, H.; Jia, W. New insights into the carboxymethyl cellulose adsorption on scheelite and calcite: Adsorption mechanism, AFM imaging and adsorption model. *Appl. Surf. Sci.* **2019**, *463*, 105–114. [[CrossRef](#)]
34. Dong, L.; Wei, Q.; Jiao, F.; Qin, W. Utilization of polyepoxysuccinic acid as the green selective depressant for the clean flotation of phosphate ores—ScienceDirect. *J. Clean. Prod.* **2020**, *282*, 124532. [[CrossRef](#)]
35. Yang, B.; Wang, D.; Cao, S.; Yin, W.; Xue, J.; Zhu, Z.; Fu, Y.; Yao, J. Selective adsorption of a high-performance depressant onto dolomite causing effective flotation separation of magnesite from dolomite. *J. Colloid Interface Sci.* **2020**, *578*, 290–303. [[CrossRef](#)] [[PubMed](#)]
36. Gao, Y.; Gao, Z.; Sun, W.; Yin, Z.; Wang, J.; Hu, Y. Adsorption of a novel reagent scheme on scheelite and calcite causing an effective flotation separation. *J. Colloid Interface Sci.* **2018**, *512*, 39–46. [[CrossRef](#)]
37. Filippova, I.V.; Filippov, L.O.; Lafhaj, Z.; Barres, O.; Fornasiero, D. Effect of calcium minerals reactivity on fatty acids adsorption and flotation. *Colloids Surf. A Physicochem. Eng. Asp.* **2018**, *545*, 157–166. [[CrossRef](#)]
38. Sanderson, R.T. Electronegativity and bond energy. *J. Am. Chem. Soc.* **1983**, *105*, 2259–2261. [[CrossRef](#)]
39. Wolsey, W.C. Chemistry of the Elements (Greenwood, N.N.; Earshaw, A.). *J. Chem. Educ.* **1985**, *62*, A133. [[CrossRef](#)]